

Poly-3-hydroxyalkanoates-co-polyethylene Glycol Methacrylate Copolymers for pH Responsive and Shape Memory Hydrogel

Ahmad Mohammed Gumel,¹ Mohamad Suffian Mohamad Annuar^{1,2}

¹Faculty of Science, Institute of Biological Sciences, University of Malaya, Kuala Lumpur 50603, Malaysia

²Centre for Research in Biotechnology for Agriculture (CEBAR), University of Malaya, Kuala Lumpur 50603, Malaysia

Gumel contributed to writing and compilation of article, established methodology, data collection, presentation, and analyses and main author of the article. Annuar contributed to establish methodology and assisted with article compilation and editing.

Correspondence to: A. M. Gumel (E-mail: gumel@um.edu.my)

ABSTRACT: Multifunctional hydrogels combining the capabilities of cellular pH responsiveness and shape memory, are highly promising for the realization of smart membrane filters, controlled drug released devices, and functional tissue-engineering scaffolds. In this study, lipase was used to catalyze the synthesis of medium-chain-length poly-3-hydroxyalkanoates-co-polyethylene glycol methacrylate (PHA-PEGMA) macromer, which was used to prepare pH-responsive and shape memory hydrogel via free radical polymerization. Increasing the PEGMA fraction from 10 to 50% (mass) resulted in increased thermal degradation temperature (T_d) from 430 to 470°C. Highest lower critical solution temperature of 37°C was obtained in hydrogel with 50% PEGMA fraction. The change in PEGMA fraction was also found to highly influence the hydrogel's hydration rate (r) from 2.8×10^{-5} to 7.6×10^{-5} mL·s⁻¹. The hydrogel's equilibrium weight swelling ratio (q_e), protein release and its diffusion coefficient (D_m) were all found to be pH dependent. Increasing the phosphate buffer pH from 2.4 to 13 resulted in increased q_e from 2 to 16 corresponding to the enlarging of network pore size (ζ) from 150 to 586 nm. Different types of cross-linker for the hydrogel influenced its flexibility and ductility. © 2014 Wiley Periodicals, Inc. *J. Appl. Polym. Sci.* **2014**, *131*, 41149.

KEYWORDS: biodegradable; biomaterials; Biopolymers and renewable polymers; composites; drug delivery systems

Received 24 February 2014; accepted 10 June 2014

DOI: 10.1002/app.41149

INTRODUCTION

The continuous increase in the utilization of nondegradable polymers has health and ecological implications, especially from biomedical and environmental perspectives. Recent advances in the use of biodegradable polymers over nondegradable ones are among the measures taken toward environmental friendliness and an increase in the sophistication of biomedical applications.

Advancement in genetic engineering and proteomics led to the production of diverse therapeutic proteins and peptides. Oral administration of these protein-based drugs usually ends up in low bioavailability, which necessitates intramuscular or intravenous administration of the drugs.¹ However, most of the proteins delivered *via* such parenteral route were also reported to be rapidly eliminated from blood circulation, demanding repeated administration to achieve a maximum therapeutic efficacy.² Thus, the growing demand for biocompatible and degradable drug carriers with controlled release triggers for efficient delivery of therapeutic drugs to the target site.

Hydrogel-based amphiphilic polymer composites containing hydrophilic and lipophilic macromers are interesting due to

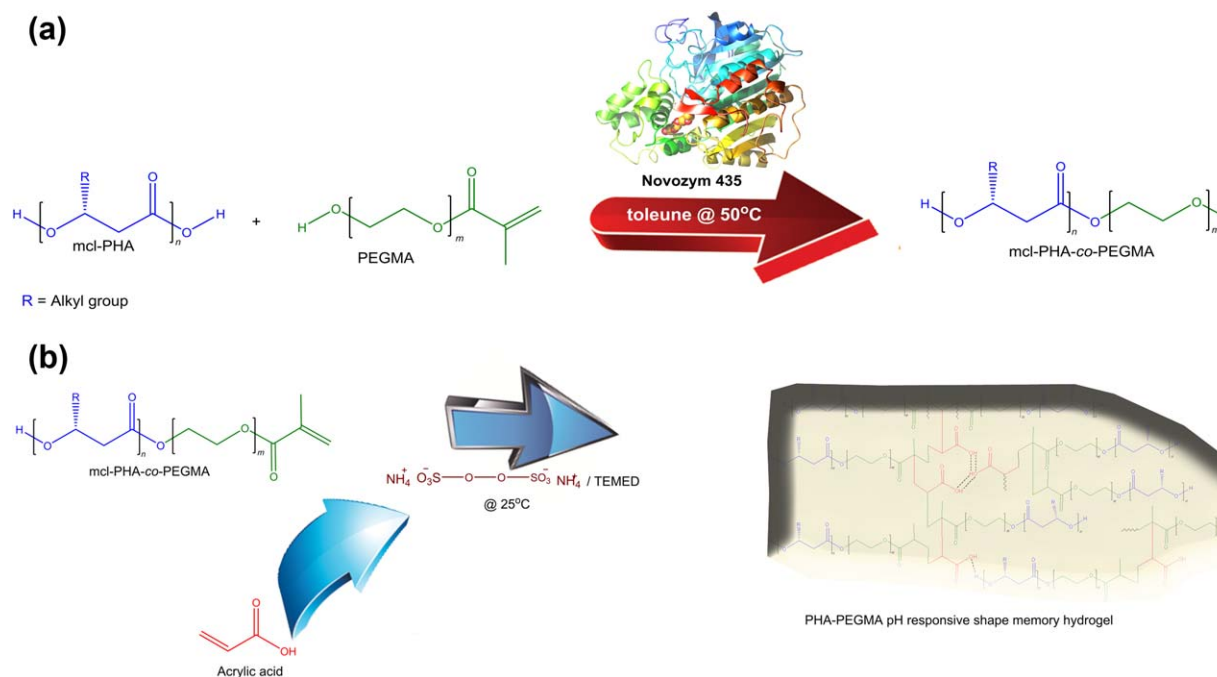
their environment-sensitive micellar properties, such as temperature and pH responsiveness, excellent biocompatibility, lack of proinflammatory effects of polymeric systems and controlled capacity in protein release.² This has potential exploitation in site-specific drug delivery devices,³ microfluidic devices,⁴ artificial muscle-like actuators,⁵ and in bioseparation or filtration.⁶

A number of polymeric-based hydrogel delivery systems for bioactive proteins have been reported, such as those composed of dextran,^{2,7} polyethylene glycol,⁸ self-assembling peptide nanofibers,⁹ hyaluronic acids,¹⁰ hydroxyethyl starch-co-poly(ethylene glycol) methacrylate,¹¹ sucrose methacrylate,¹² polysaccharide,¹³ and poly(caprolactone-co-N-isopropylacrylamide).¹⁴ Hydrogels of polymeric composites containing biocompatible medium chain length polyhydroxyalkanoates (mcl-PHAs), polyamide and/or polyamino acids are known to have biomimetic properties especially in cell adhesion or targeting and their efficacy is well distinguished in cancer biology and innate immunity.¹⁵

Despite the reported bioresorbability, compatibility, and degradability of bacterial PHAs, relatively less investigation on PHA composite hydrogels were documented.¹⁶ Those literature that

Additional Supporting Information may be found in the online version of this article.

© 2014 Wiley Periodicals, Inc.



Scheme 1. (a) Enzymatic synthesis of PHA-PEGMA macromer; (b) PHA-PEGMA hydrogel synthesis *via* free radical polymerization. [Color figure can be viewed in the online issue, which is available at wileyonlinelibrary.com.]

reported the synthesis of such polymeric composites and their hydrogels, used highly crystalline poly-3-hydroxybutyrate (PHB) as copolymeric macromer *via* conventional chemical catalysis to produce the copolymeric macromer using 4-(dimethylamino)pyridine (DMAP) as catalyst in the presence of potent allergen *N,N*-dicyclohexylcarbodiimide (DCC) as initiator. It is well known that DCC can cause lung edema and skin dermatitis, while the product of catalyst-initiator complex (dicyclohexylurea)¹⁷ is known to be a potent inhibitor to soluble epoxide hydrolase,¹⁸ an important enzyme in xenobiotic metabolism as well as the metabolism of endogenous signaling molecules such as epoxyeicosatrienoic acids.

In this study, we reported for the first time the utilization of excellent enantiomeric selectivity, specificity and catalytic activity of Novozym 435 to synthesize composite polymeric macromer of medium chain length PHA-polyethylene glycol methacrylate (PHA-PEGMA) under mild reaction conditions, thereby eliminating the use of DMAP and its initiator. Furthermore, to the best of our knowledge, currently there is no report on the use of medium chain length bacterial PHA as copolymeric component in pH responsive and shape memory hydrogel formulation.

EXPERIMENTAL

Materials

Novozyme[®] 435, PEGMA ($M_n = 526$ Da), acrylamide, azobisisobutyronitrile, *N,N,N',N'*-tetramethylethylenediamine (TEMED), pyridine-D, ammonium persulfate (APS), ethylene diamine, and (3-[4,5-dimethylthiazol-2-yl]-2,5-diphenyltetrazoliumbromide (MTT) were purchased from Sigma Aldrich. Acrylic acid, 1,1,4,7,10,10-hexamethyltriethylenetetramine, methylene diacrylamide, chloroform-D, and other organic solvents used were

purchased from Merck. Analytical grade chemicals were used throughout the study. Human liver embryonic cells, HeLa derivative (WRL68) was purchased from American Type Culture Collection (ATCC), and was used as a model cell line to evaluate the cytotoxic effect of the synthesized hydrogel.

Biodegradable mcl-PHA ($M_w \approx 56$ kDa, $M_n \approx 13.6$ kDa) with comonomeric composition of $C_6 : 0$ to $C_{14} : 0$ was obtained from bacterial fermentation as previously reported,^{19,20} using *Pseudomonas putida* Bet001 as producer microorganism and hexadecanoic acid as a sole carbon and energy source.

Methodology

Enzyme Activity. The enzymatic activity is assayed as reported previously.²⁰ In brief, Novozym 435 (100 mg) was added to a vial containing 10 mL of a 10 mM 4-nitrophenyl palmitate solution in *n*-hexane. To this mixture 60 μ L of 1M absolute ethanol was added. The resulting slurry was incubated at 40°C, 200 rpm for a period of 20 min. Aliquots (30 μ L each) of the reaction mixture were withdrawn at intervals and quenched by mixing with 1 mL of 0.1 M NaOH in a quartz cuvette. The 4-nitrophenol liberated by the reaction was measured at 412 nm (UV-Vis spectrophotometer V-630; Jasco, Japan) against distilled water as blank. The enzyme activity was calculated as the slope of a plot of 4-nitrophenol released versus time.

Enzymatic Synthesis of PHA-PEGMA Macromer. PHA (1.0 g) was dissolved in 10 mL toluene in a 20-mL capped reaction vial, PEGMA (40%, v/v reaction solvent) was then added. To this mixture, 100 mg Novozym[®] 435 lipase was added and incubated under constant stirring in an oil bath at 50 (± 1)°C, 200 rpm for 48 h [Scheme 1(a)]. The synthesized macromer was extracted from the crude reaction mixture by filtering the immobilized enzymes using Buchner filter system, followed by

evaporating the filtrate to dryness under vacuum. Then it was dissolved in 3.0 mL tetrahydrofuran (THF) and precipitated in 20 mL of cold *n*-heptane (4°C). The solvent was then decanted and the precipitate was re-purified by further subjecting it to three-cycle precipitation. At each stage, the macromer precipitate was dissolved in THF (2.0 mL) and then added to cold *n*-heptane (15 mL, 4°C). Finally, the beige-colored precipitate of the macromer (~90%) was recovered and dried *in vacuo* over phosphorus pentoxide before analytical characterization. All reaction steps were carried out as described for other studies such as the effect of PEGMA loading amount (10–50%, w/w).

Synthesis of PHA-PEGMA Hydrogel. The PHA-PEGMA hydrogel was synthesized by free radical polymerization [Scheme 1(b)]. A solution of PHA-PEGMA macromer (GPC $M_w = 67,800$ Da) was prepared by dissolving the macromer (100 mg) in 0.5 mL chloroform and mixed with 1.5 mL of 50 mM physiological phosphate buffer (pH 7). Acrylic acid (200 μ L) was added as a crosslinker and to promote inter-polymer complexation by hydrogen bond. The mixture was sparge with nitrogen gas for 5 min. 120 μ L APS and 100 μ L of 20% (v/v) TEMED (as a free radical initiator) was subsequently added under nitrogen atmosphere. Thereafter the reaction mixture was quickly withdrawn into 1 mL hypodermic syringe (5 mm internal diameter) as a mold and allowed to polymerize at 25°C for 1 h. The hydrogel was recovered from the syringe by slicing the top end of the syringe, then using the plunger to push the hydrogel out into a Petri dish containing 30 mL deionized water and allowed to immerse for 5 days. The water was freshly changed every day to remove organic solvents and unreacted chemicals. After the fifth day, the hydrogel was removed and dried under vacuum over phosphorus pentoxide. All reactions were carried out as mentioned except stated otherwise.

Preparation of Protein-Loaded PHA-PEGMA Hydrogels. The protein-loaded PHA-PEGMA hydrogels were prepared using phosphate buffer that contains 50 μ g·mL⁻¹ bovine serum albumin (BSA) and polymerized as mentioned previously. To study protein release, vacuum dried protein loaded hydrogels were cut into pieces of about 5.0 ± 0.2 mm long each. The gels were then weighed and totally immersed in 50 mM phosphate buffer solution (10.0 mL) of different pH (2.4–13). These gels were allowed to stand at room temperature for 48 h (1 atm, $25 \pm 1^\circ\text{C}$, 87% relative humidity). At regular interval, the released protein concentration as a function of medium pH was evaluated using standard Bradford assay as reported elsewhere.^{21,22} The swelling ratio of the hydrogel was evaluated by measuring the weight of the gels periodically.

Product Characterization

¹H-NMR and Fourier-Transfer Infrared Analyses. Proton NMR spectra were recorded on a JEOL JNM-GSX 270 FT-NMR (JOEL, Tokyo, Japan) machine at 250 MHz according to reported literature.²³ Perkin-Elmer Fourier-Transfer Infrared (FTIR) RX 1 spectrometer (Perkin-Elmer, Wellesley, MA) was used to record FTIR-ATR spectra of PHA-PEGMA macromer and the hydrogel as previously reported.²³

Thermometric Analyses. Differential scanning calorimetric (DSC) analysis of the PHA-PEGMA macromer and the hydrogel

were performed on Perkin-Elmer Diamond DSC instrument using HyperDSC[®] technique (Perkin-Elmer). About 4 mg of each sample was immerse in 50 mM phosphate buffer (pH 7) and were allowed to equilibrate at 4°C for 24 h before the analysis. Scans were observed over the temperature range of 30–100°C at heating and cooling rate of 5°C min⁻¹ in nitrogen flow rate of 50 mL min⁻¹. The DSC microcalorimetric analysis was used to determine the lower critical solution temperatures (LCST) of the hydrogels as reported elsewhere.²⁴

Thermogravimetric analysis (TGA) was performed on a Perkin-Elmer TGA4000 instrument (Perkin-Elmer). The samples were heated from 30 to 900°C at a rate of 10°C min⁻¹ in nitrogen gas flow rate of 20 mL min⁻¹.

GPC Analysis. Gel permeation chromatography of the PHA-PEGMA macromer was recorded on Waters 600 (Waters Corp, Milford, MA) equipped with a Waters refractive index detector (model 2414) and the following gel columns (7.8 mm internal diameter \times 300 mm each) in series: HR1, HR2, HR5E and HR5E Waters Styrogel HR-THF. Monodisperse polystyrene of different molecular weights (3.72×10^2 , 2.63×10^3 , 9.10×10^3 , 3.79×10^4 , 3.55×10^5 , 7.06×10^5 , 3.84×10^6 , and 6.77×10^6 Da) was used as standards to produce the calibration curve. The polymer samples (2.0 mg mL⁻¹) were dissolved in THF, filtered through a 0.22 μ m PTFE filter and then injected into the GPC (100 μ L) at 40°C. Tetrahydrofuran was used as mobile phase at flow rate of 1.0 mL min⁻¹.

MTT Assay. The cytotoxic effects of the synthesized hydrogel and its leachable products was evaluated using MTT assay according to reported method²⁵ with adoption of minor modification. Briefly, different sizes of the synthesized hydrogel weighing (0.1–2.5 g) were cut and dried *in vacuo*. The dried hydrogels were then sterilized using ultraviolet light for 5 min in a laminar flow, and each was placed in a well of 12-well plates containing 2 mL of RPMI 1640 growth medium, while another triplicate wells were left without the immersion of the hydrogel serving as control. All these samples were then incubated in 5% CO₂ incubator at 37°C in a 95% relative humidity for 48h to allow for the leachable chemicals to leach into the medium. After the leaching period, the hydrogels were carefully removed and the wells were then aseptically seeded with confluent cultured WRL68 cells at a seeding density of 10×10^3 cells/well, and the whole culture plates were incubated in 5% CO₂ incubator at 37°C and 95% relative humidity for 48 and 72 h, respectively. Immediately after the incubation time, 100 μ L of MTT solution (5 mg mL⁻¹ PBS) was added to each well and incubated at 37°C for another 4 h under constant gyration. Thereafter, dimethyl sulfoxide (200 μ L) were added to the cultures and mixed thoroughly to dissolve the dark blue crystals of formazan. And the chromogenic formazan was photometrically quantified at 570 nm according to reported procedures.^{26,27}

Calculations. The hydrogel weight swelling ratio (q) is given by the weight ratio of the swelling gel to that of the dry gel as shown in the following equation:

$$q = \frac{W_s}{W_d} \quad (1)$$

The equilibrium weight swelling ratio (q_e) is given by the following equation:

$$q_e = \frac{W_s - W_d}{W_d} \quad (2)$$

where W is the weight of the swelling (s) and dry (d) gel, respectively.

In a dry hydrogel, the rate (r) of solvent uptake with time (t) is given by eq. (3) as previously reported²⁸:

$$r = k \cdot t^n \quad (3)$$

hence,

$$\log r = \log k + n \log t \quad (4)$$

where k is the rate constant and n is the diffusional exponent relating the time dependence of solvent uptake. At $n = 0.5$ relaxation does not affect solvent transport in Fickian diffusion. However, when $n = 1$ indicates hydrogel's relaxation limits the solvent transport in Fickian diffusion.²⁸

The hydrogel hydration percentage ($H\%$) is calculated according to Vieira et al.¹³ as given in the following equation:

$$H\% = \left(1 - \frac{1}{q}\right) \times 100 \quad (5)$$

The volume swelling ratio (v') is defined as the ratio of the volume of swollen gel to that of dry gel as denoted by the following equation:

$$v' = \frac{v_s}{v_d} \quad (6)$$

Both swollen and dry gel volumes were calculated according to eqs. (7) and (8), respectively:

$$v_s = \frac{W_{s,a} - W_{s,h}}{\rho_h} \quad (7)$$

$$v_d = \frac{W_{d,a} - W_{d,h}}{\rho_h} \quad (8)$$

where W_s and W_d are respective weights of swelling and dry gels in air (a) and n -heptane (h), and ρ_h is n -heptane density.

Among the important parameters used in hydrogels characterization is the mesh size (ξ),²⁹ as given in the following equation:

$$\xi = (v_{i,s})^{-1/3} \cdot \sqrt{r_0^{-2}} \quad (9)$$

where $(v_{i,s})^{-1/3}$ is the elongation ratio denoted by eq. (10) as reported earlier²⁸ and $\sqrt{r_0^{-2}}$ is the average distance between two adjacent crosslinks as given by eq. (11)³⁰:

$$v_{i,s} = \frac{1}{v'} \quad (10)$$

$$\sqrt{r_0^{-2}} = l \cdot \sqrt{M_n} \quad (11)$$

where $v_{i,s}$ is the polymer volume fraction after equilibrium swelling and l is the bond-length along the polymer backbone, and is given by 0.15 nm in vinyl polymers.²⁹

Taking the cylindrical geometry of the syringe mold, the protein released by the hydrogels were evaluated based on diffusion coefficients using free volume theory according to the following equation as reported previously:³⁰

$$\ln\left(\frac{D_m}{D_o}\right) = \ln(\Phi) - \left(\frac{kr^2}{V_{f,\text{water}}}\right) \cdot \left(\frac{1}{H} - 1\right) \quad (12)$$

where D_o is the diffusion coefficient of the protein in water given by eq. (13), D_m is the protein diffusion coefficient in the hydrogel matrix described by eq. (14), Φ denotes the screening effect of hydrogel networks, r is hydrodynamic radius of the protein, $V_{f,\text{water}}$ is free volume in water, k is a constant, and H is hydrogel hydration.

$$D_o = \frac{k_B T}{3\pi\eta d} \quad (13)$$

$$\frac{[P_t]}{[P_o]} = 4 \cdot \sqrt{\frac{D_m t}{\pi r^2}} \quad (14)$$

where k_B is Boltzmann constant, T is absolute temperature, η is solvent viscosity, d is protein hydrodynamic diameter, $[P_t]$ is released protein concentration at time (t), $[P_o]$ is initial protein concentration, and r is the hydrogel radius at the equilibrium state. For BSA, a D_o value of $0.59 \times 10^{-6} \text{ cm}^2 \cdot \text{s}^{-1}$ has been reported.^{30,31}

RESULT AND DISCUSSIONS

Characterization of Polymeric Macromer and Hydrogel

In this study, using microaqueous medium, Novozym[®] 435 was successfully used for the trans-esterification of PEGMA and the bacterial medium chain length PHA under mild reaction conditions. Figure 1(a) showed the ¹H-NMR spectrum of the synthesized PHA-PEGMA macromer. In reference to internal standard tetramethylsilane, chemical shifts (a and b) were assigned to β -protons of terminal methyl groups ($\text{CH}_3\text{-CH}_2\text{-}$ and $\text{CH}_3\text{CHO-}$) in the PHA macromer side-chain, respectively. Chemical shifts (c and d) were assigned to α,β -protons of methylene groups ($\text{CH}_2\text{-CH}_2\text{-}$ and $\text{CH}_2\text{-CHO-}$) in the PHA macromer side-chain. Chemical shifts (e and e') were assigned to ethylene group *cis* and *trans* protons $\text{CH}_3\text{-CH=CH}_2$ in the methacrylate macromer. Chemical shifts (f , g , and h) were assigned to α , β -protons of the methylene groups ($\text{-OCH-CH}_2\text{-COO-}$) in the PHA macromer. Chemical shifts (i , j , l , and l') were assigned to α,β -protons in methylene groups of polyethylene glycol macromer backbone (O-CH_2 , COO-CH_2 and $\text{O-CH}_2\text{-CH}_2\text{-}$). Chemical shift (m) was assigned to terminal methyl α -protons in $\text{CH}_3\text{(C(=O)R)CH=CH}_2$ in the methacrylate macromer. Chemical shift (k) was assigned to α,β -protons ($\text{-OCH-CH}_2\text{-COO-}$) of methane groups in the PHA macromer. This assignment was found to be in accordance with previously reported literatures.^{32,33}

The attenuated total reflectance FTIR spectra of PHA-PEGMA macromer and the hydrogel were presented in Figure 1(b). The absorption band at 1724 cm^{-1} was attributed to the ester (C=O) stretching vibration as reported in literature.^{33,34} Absorptions at $1258\text{--}1140 \text{ cm}^{-1}$ were assigned to ester (C-C(O)-C) stretching vibrations.³³ In the PHA-PEGMA macromer spectrum, the absorption at 1624 cm^{-1} was attributed to

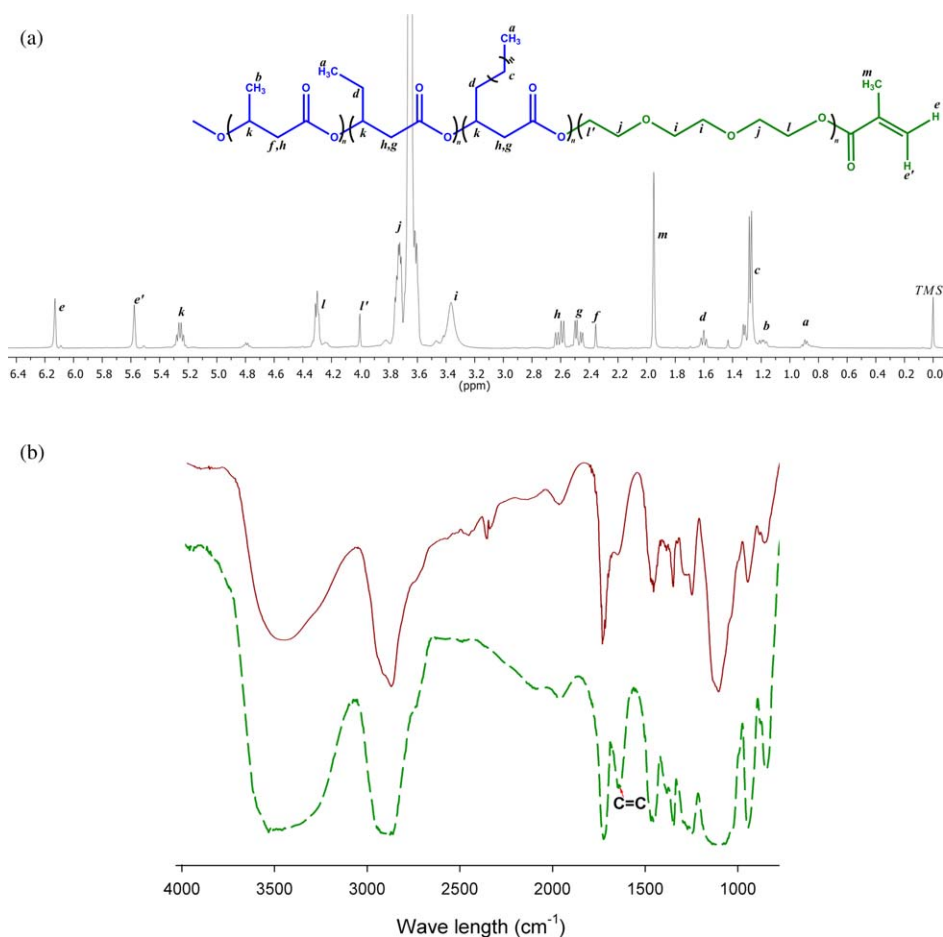


Figure 1. (a) Proton NMR spectrum of the PHA-PEGMA macromer; (b) FTIR spectra of PHA-PEGMA macromer (---) and the hydrogel (—). [Color figure can be viewed in the online issue, which is available at wileyonlinelibrary.com.]

the presence of conjugated stretching vibration of ethenyl group (C=C) in the PEGMA copolymer.³⁵ Interestingly, this seems to disappear in the PHA-PEGMA hydrogel spectrum [Figure 1(b)], indicating almost total crosslinking of the macromer.

In Vitro Cytotoxicity Test

The cytotoxicity of the synthesized hydrogel's leachable products was evaluated following MTT reduction assay using Human HeLa cell derivative (WRL68) as a cellular model. Reference to the control sample [Figure 2(a,b)], the results demonstrate there is a nonsignificant decrease in cell viability with the increasing size of the hydrogel used even at 72 h of incubation (96% cell viability at 2.5 g hydrogel extract). Thus, from this observations (Figure 2), it is considered that the synthesized hydrogel has no cytotoxic effect on normal WRL68 cell line even at higher weight load of 2.5 g. This observation was found to be in accordance with similar observation of higher cellular viability >80% upon testing hydrogel's toxicity were reported.^{27,36,37}

Effect of PEGMA Loading Amount on Hydrogel Thermal Stability and LCST

The effect of PEGMA loading amount (10–50%, w/w) during macromer synthesis on the thermal stability of the prepared hydrogel was studied using TGA and DSC analyses. It was found that there was a correlation between the amount of PEGMA

loaded and the thermal degradative stability of the hydrogel, such that increased PEGMA concentration during macromer synthesis resulted in gradual increase in the thermal degradation temperature (T_d) of the respective hydrogel (Figure 3). For example, T_d of 430°C was observed in hydrogel obtained from macromer that was synthesized at 10% PEGMA. Changing the PEGMA loading to 30% resulted in macromer that yields hydrogel with T_d of about 454°C. This increased to 470°C in hydrogel with 50% PEGMA content (Figure 3). The increase in thermal stability with increasing PEGMA content could be due to the increase in macromer molecular weight with PEGMA content (Table I). Variability in the loading amount of PEGMA during macromer synthesis not only resulted in hydrogels of varying thermal stability, but also changes several parameters, specifically free radical concentration along the gelation time.³⁸ Similar increase in thermal stability with increasing comonomer content was reported in PHB-NIPAAm triblock macromer,³⁹ PHB-PEO triblock copolymers⁴⁰ and in pH responsive chitosan-poly(*N*-2-hydroxy-ethyl-DL-aspartamide) composite hydrogels.⁴¹

The DSC microcalorimetric analysis was used to determine the LCSTs of the hydrogels. The onset temperature was determined from crossing of the baseline with the leading edge of the endotherm as reported by Zhang and Chu.⁴² Generally, an average LCST of 33 ($\pm 2^\circ\text{C}$) was observed in the hydrogels. This

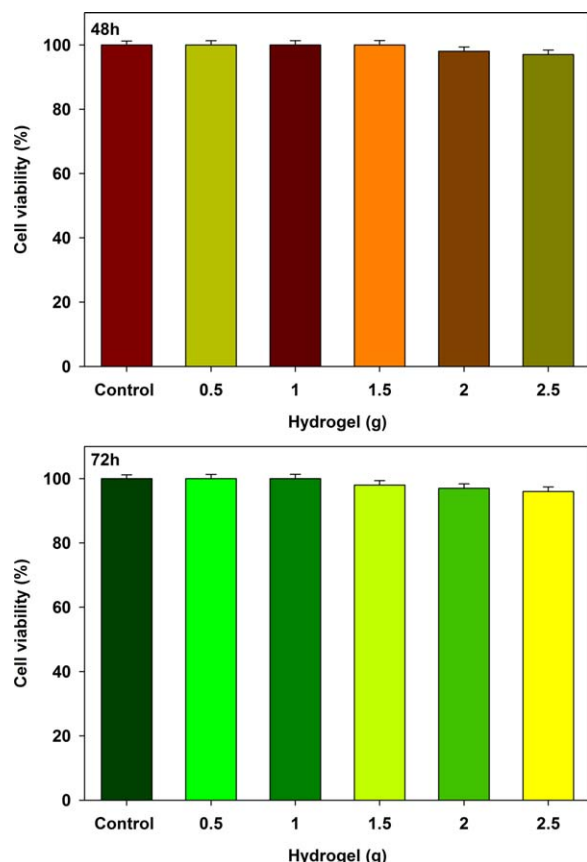


Figure 2. MTT cytotoxicity assay of the synthesized hydrogel at different hydrogel mass. [Color figure can be viewed in the online issue, which is available at wileyonlinelibrary.com.]

observation was also found to agree well with reported LCST value of 34.7°C in PEGMA composites.⁴³ The LCST of polymers is reported to be influenced by several parameters, such as the macromolecular chemical structure, molecular weight and polydispersity index.⁴³ When the amount of PEGMA loading was increased during the synthesis of the hydrogel, an increase in the LCST from 29.1°C to the physiological temperature

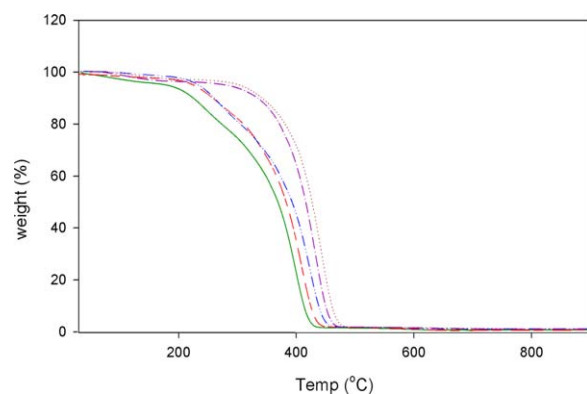


Figure 3. Hydrogel thermal stability as a function of comonomer concentration [PEGMA (w/w): 10% —, 20% ---, 30% - · -, 40% ···, and 50% - - - -]. [Color figure can be viewed in the online issue, which is available at wileyonlinelibrary.com.]

Table I. Comonomer Loading as a Function of Macromer M_w and LCST (Maximum Standard Error $\pm 5\%$)

PEGMA (%)	$M_n, \times 10^3$	$M_w, \times 10^3$	PDI	LCST (°C)
10	0.9	1.5	1.7	29.1
20	2.5	4.2	1.7	30.2
30	3.9	5.6	1.4	32.1
40	6.2	10.4	1.7	36.2
50	8.3	12.9	1.5	37.1

(37.1°C) was observed. The highest LCST at 37.1°C was obtained in hydrogel with 50% PEGMA content (Table I). There was a significant increase in LCST with increasing macromer molecular weight (Table I). This observation corroborates the earlier report that well controlled synthesis of polymers (having low polydispersity indices) exhibits sharper LCST transition.⁴⁴ Furthermore, hydrophilic-lipophilic balance of the copolymer is said to highly influence the hydrogel LCST.⁴³ Hence, increase in the hydrophilic PEGMA content resulted in a concomitant increase in LCST. These observations were found to be in accordance with Fournier et al.⁴³ studies, that reported an increase in LCST with increasing PEGMA weight % in P(DMAEMA-*stat*-PEGMA) macromer synthesized by reversible addition fragmentation chain transfer.

pH Responsive Effect on Hydrogels Equilibrium Swelling Ratio and Protein Release

The pH responsive behavior of PHA-PEGMA hydrogel was studied in phosphate buffer solution of different pH (Table II). It was found that the gel's swelling behavior is pH dependent [Figure 4(a)], increase in buffer pH resulted in the corresponding increase in hydrogels pore size [Figure 4(b)], thus incurring the progressive increase in protein release with time [Figure 4(c)]. In acidic pH of 2.4, which is below the reported methacrylic acid pK_a (4.65–5.86),⁴⁵ about 0.6 $\mu\text{g}\cdot\text{mL}^{-1}$ BSA was observed to be released within the first hour. This increased to a maximum of about 17 $\mu\text{g}\cdot\text{mL}^{-1}$ within a period of 10 h. In contrast to this observation, changing the pH to neutral condition, the protein release was observed to increase to a maximum value of $\approx 21 \mu\text{g}\cdot\text{mL}^{-1}$ after 10 h, and a maximum of $\approx 28 \mu\text{g}\cdot\text{mL}^{-1}$ in alkaline pH of 13. This was attributed to the presence of dynamic ionizable moieties in the copolymeric networks, making PHA-PEGMA hydrogel to be mechanically responsive to the change in the surrounding's concentration of hydrogen ion. The high tendency of hydrogen bond formation between the methacrylic-carboxylic acid groups and the oxygens of copolymeric macromers in the network, helps to explain their polybasic protonations at lower pH.⁴⁶ It has been reported that, in acidic buffers, i.e., pH lower than the methacrylic acid pK_a , the PEGMA carboxylic acid groups are nonionizable and the copolymeric components were able to form hydrogen bonds due to protonations.⁴⁶ This fashioned interpolymer complexes resulted in the collapse of crosslinked network. In alkaline pH, the carboxylic acid groups were ionized, leading to the dissociation of interpolymer complexes due to electrostatic repulsion. Hence swelling of the hydrogel as shown in Figure 3(a), resulting in higher protein release [Figure 4(c)]. This hypothesis is

Table II. The Influence of Buffer pH on Hydrogel's Mesh Size (ξ) and Hydration Parameters (Maximum Standard Error $\pm 5\%$)

pH	v'	$\xi, \times 10^2$ (nm)	q_e	$H\%$	$k, \times 10^{-5}$ (s $^{-1}$)	$D_m, \times 10^{-5}$ (cm 2 s $^{-1}$)
2.4	52	1.5	2	26	2.6	1.4
4.4	62	2.3	5	64	3.3	1.6
7.0	75	2.9	6	72	4.7	1.8
10	83	3.7	8	85	6.1	2.2
13	91	5.7	12	94	8.9	2.7

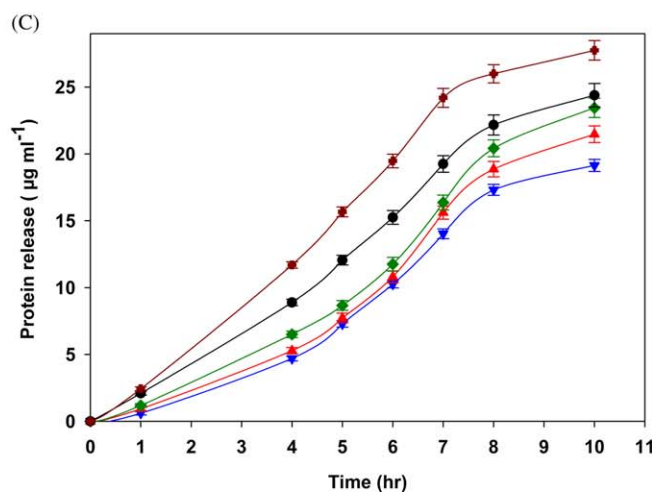
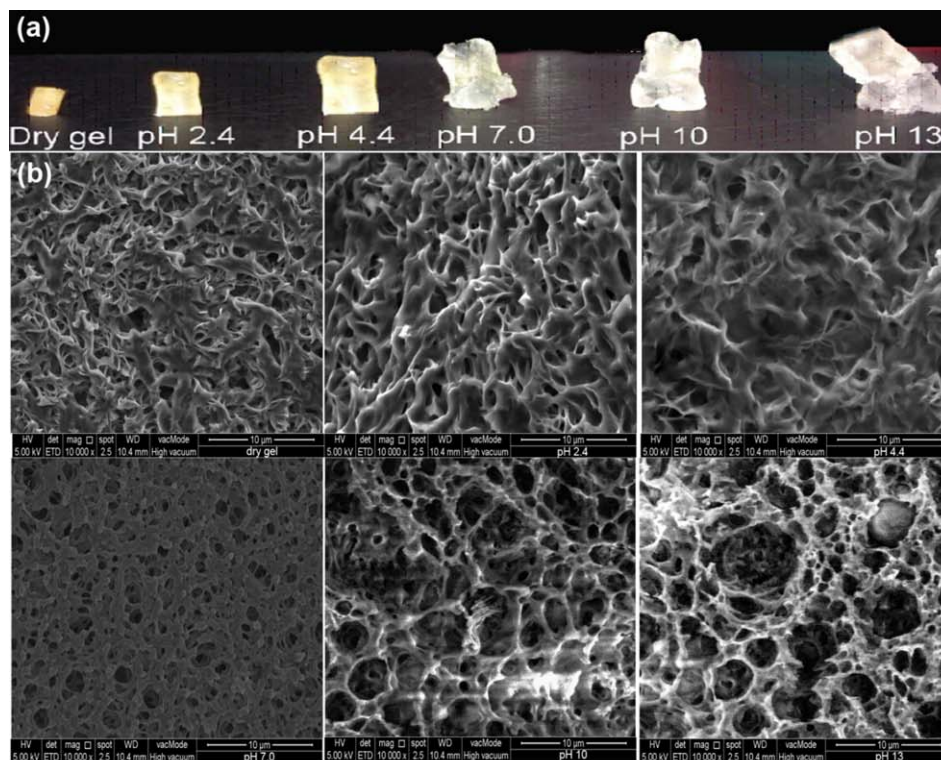


Figure 4. (a) pH dependence of hydrogel swelling volume (b) FESEM micrographs of the corresponding hydrogels. (c) Buffer pH as a function of hydrogel's protein release; pH 2.4 ▼, 4.4 ▲, 7.0 ◆, 10 ●, and 13 +. [Color figure can be viewed in the online issue, which is available at wileyonlinelibrary.com.]

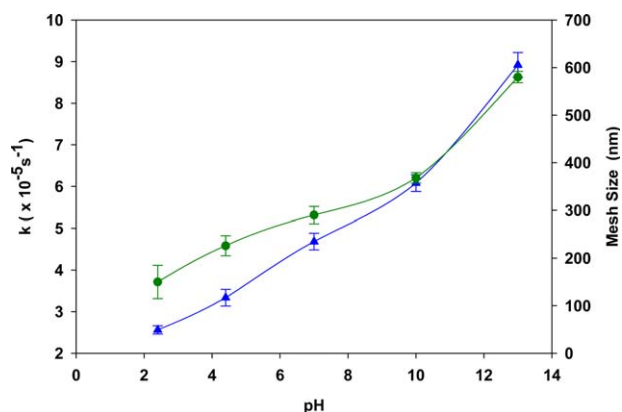


Figure 5. Influence of buffer pH on 50% PEGMA hydrogel's solvent uptake rate constant (\blacktriangle) and mesh size (\bullet). [Color figure can be viewed in the online issue, which is available at wileyonlinelibrary.com.]

further substantiated by the observed increase in the equilibrium weight swelling ratio (q_e) from 2 to 16; and the corresponding increase in protein diffusion coefficient (D_m) from 1.4 to 2.7 $\text{cm}^2\cdot\text{s}^{-1}$ with increasing buffer pH from 2.4 to 13 (Table II). Similar observations on increasing hydrogel weight swelling ratio with the increase in buffer pH were reported.⁴⁶ During the synthesis of pH responsive hydrogel of polymethacrylic acid grafted polyethylene glycol, Torres-Lugo and Peppas⁴⁷ reported an increase in equilibrium weight swelling ratio from about 1.8 to 14 with buffer pH from 3.1 to 8.3.

Influence of Buffer pH on Hydrogel's Hydration Rate Constant and Mesh Size (ξ)

The hydrogel's hydration level plays a role in the control of mesh size (ξ) and screening of the solute particles that pass through.³⁰ The increase in PEGMA carboxylic acid ionization with increasing alkalinity of the buffer resulted in observed enlargement in calculated network mesh size (Figure 5). This in turn resulted in an increase in percentage hydration (Table II). Increasing the buffer pH from 2.4 to 10, the mesh size was found to enlarge from 150 nm to 368 nm reaching a maximum size of 586 nm in alkaline pH of 13. Over this pH range, the rate constant (k) for solvent uptake was also found to increase

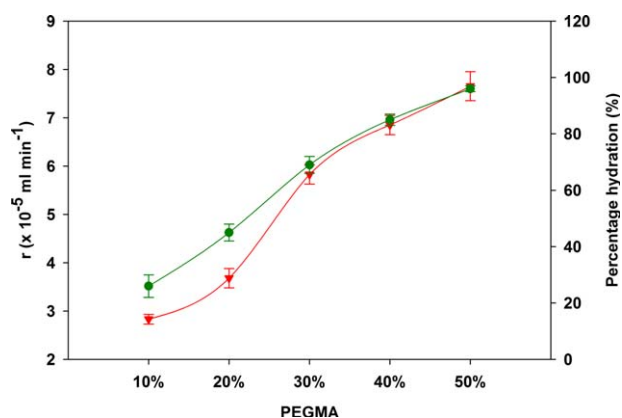


Figure 6. PEGMA loading as a function of hydrogel's solvent uptake rate (\blacktriangledown) and percentage hydration (\bullet) at pH 7. [Color figure can be viewed in the online issue, which is available at wileyonlinelibrary.com.]

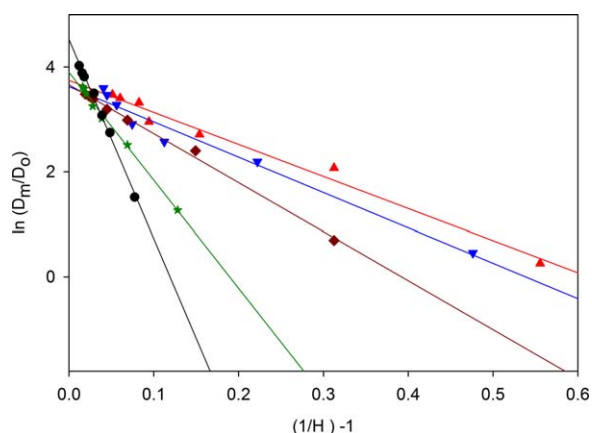


Figure 7. Linearized diffusion coefficient of protein in PHA-PEGMA hydrogels (10% PEGMA \blacktriangle , 20% PEGMA \blacktriangledown , 30% PEGMA \blacklozenge , 40% PEGMA \blackstar , and 50% PEGMA \bullet). [Color figure can be viewed in the online issue, which is available at wileyonlinelibrary.com.]

from 2.6 to $8.9 \times 10^{-5} \text{ s}^{-1}$, corresponding to the observed increase in percentage hydration ($H\%$) from 26 to 94% (Table II). As expected, the hydrogel's pH dependence of protein release rate [Figure 4(c)] is in agreement with the hydration rate (Table II). At lower hydration rate, lower protein release rate was observed and *vice versa*. Similar observations were reported by Hennink et al.³⁰ on the influence of water content on BSA release in glycidyl methacrylate-dextran hydrogels. Possible explanation to this observation could be attributed to the earlier mentioned protonation complexation by hydrogen bonding at lower pH and the ionization decomplexation at higher pH.

Influence of PEGMA Loading Amount on Hydrogel's Hydration Rate and Protein Release

The rate of protein release in a matrix system was reported to be largely dependent on the hydration rate of the polymeric materials, which is influenced by the hydrophilic-lipophilic nature of the macromolecular materials, and this can be studied using free volume theory as depicted in equation (12).³⁰ Figure 6 showed the rate of solvent uptake as a function of PEGMA weight percentage loaded. As expected, the rate of water uptake (r) was observed to be lowest ($2.8 \times 10^{-5} \text{ mL}\cdot\text{s}^{-1}$) in a macromer synthesized from 10% PEGMA and highest ($7.6 \times 10^{-5} \text{ mL}\cdot\text{s}^{-1}$) in macromer of 50% PEGMA. This observation was found to correspond with the percentage hydration of 26% in 10% PEGMA and 96% in hydrogel with 50% PEGMA loading, respectively. In the absence of particulate screening effect from either the hydrogel's mesh size or solvent uptake, free volume theory showed a linear relationship in the plot of normalized protein diffusion coefficients.³⁰ As shown in Figure 7, the protein diffusion in hydrogels with lower PEGMA loading (10–20%) was observed to deviate from the free volume theory prediction. On the other hand, hydrogels obtained from higher PEGMA loading (30–50%) showed excellent conformity with the prediction in terms of protein release. In general, the protein diffusion agreed well with the free volume theory at higher hydration level and deviates at lower level. For example, in both hydrogels of lower PEGMA loading (Figure 7), the protein

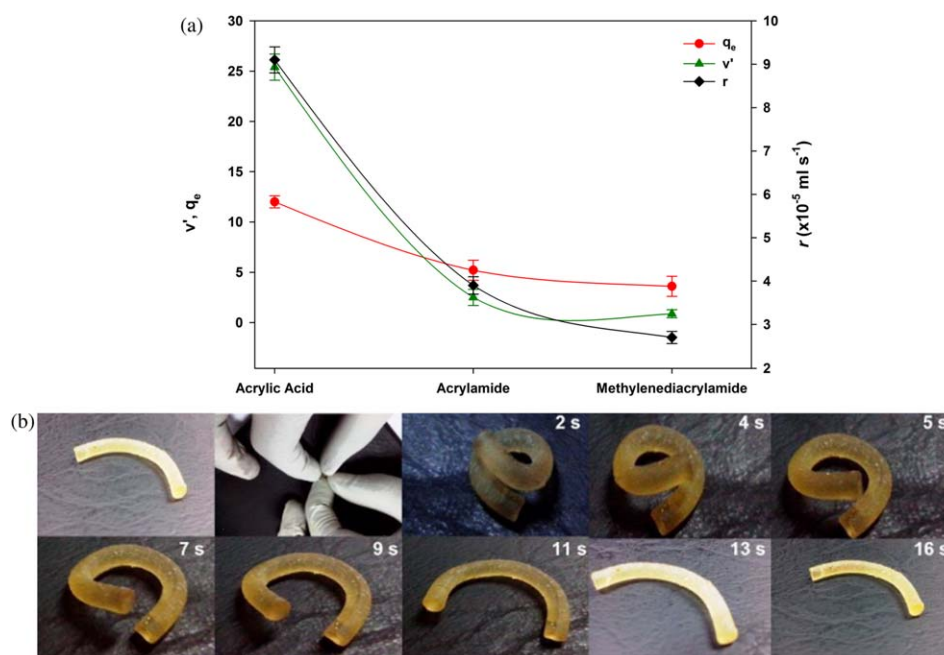


Figure 8. (a) Hydrogel's crosslinker type as a function of equilibrium weight swelling ratio (●), volume swelling ratio (▲), and rate of solvent uptake (◆). (b) Shape memory of acrylic acid crosslinked PHA-PEGMA hydrogel. [Color figure can be viewed in the online issue, which is available at wileyonlinelibrary.com.]

screening effect appeared to set-in at lower hydration level [i.e., higher $(1/H - 1)$ values ≈ 0.25] corresponding to the observed hydration rate constant of $\approx 3.0 \times 10^{-5} \text{ s}^{-1}$. This observation could be attributed to the reported hydrophobic and hydrogen bonding interactions between the BSA and the network's highly dense-crosslink at lower hydration level, which could limit the protein release.³⁰

Effect of Crosslinker Type on Hydrogel Solvent Absorption Rate and Ductility

Previous research has documented that the mechanism of protein release in hydrogels network polymers is influenced by a variety of factors, including the type of crosslinker and crosslink density.⁴⁸ The effect of crosslinking type on solvent absorption in PHA-PEGMA hydrogel has been studied using acrylic acid (AAc), acrylamide (AAM) and *N,N*-methylene-diacrylamide (MDA) under neutral pH [Figure 8(a)]. In all the hydration analyses, crosslinking using acrylic acid was observed to yield higher equilibrium weight swelling ratio ($q_e = 12$), volume swelling ratio ($v' = 25$) and rate of solvent uptake ($r = 9.1 \times 10^{-5} \text{ mL}\cdot\text{s}^{-1}$) as compared to AAM with values of $q_e = 5.2$, $v' = 2.5$ and $r = 3.9 \times 10^{-5} \text{ mL}\cdot\text{s}^{-1}$. In comparison to the two crosslinkers, MDA a dicrosslinker agent was found to exhibit the lowest values for q_e , v' and r for all the three crosslinking agents tested [Figure 8(a)]. This decrease in hydration parameters in acrylamides crosslinked hydrogels could be due to reported low protonation of the NH_2 of the amide group at higher pH.⁴⁹ The compaction of the crosslinked complexes resulted in decreased equilibrium weight swelling ratio and subsequent reduction in both rate of solvent uptake and volume swelling ratio, respectively. This further explained the observed reduction

of both parameters in MDA hydrogel sample [Figure 8(a)], due to the presence of two acrylamide crosslinkers. Jagadish and Vishalakshi⁴⁹ reported similar observation in inter-penetrating polymer networks of guar-gum and polyacrylamide.

In studying the influence of crosslinking agents on the hydrogel ductility, we found that acrylic acid crosslinked hydrogels were more flexible to the extent that can be twisted spirally and returned to its initial shape within a short period of time [Figure 8(b)]. In fact, the hydrogel was observed to regain its initial shape in less than 20 s at ambient temperature ($25 \pm 1^\circ\text{C}$) as shown in the media file (Supporting Information 1). In contrast to this observation, all the acrylamide crosslinked hydrogels were found to be rigid and showed high resistance to mechanical force applied. A possible reason for this resistance is the high interaction *via* hydrogen bonding among the NH_2 of the amide groups in the acrylamide. Thus promoting the collapse of the complexes, this resulted in the rigidity of the hydrogel. Hence, higher number of crosslinkers in the polymer networks augments the resistance of the hydrogel toward mechanical deformation. This was found to be in agreement with reported observation on the swelling effect toward pH-responsive hydrogel's mechanical properties.⁴

CONCLUSIONS

PHA-PEGMA macromer was successfully transesterified using enzymatic catalysis. Based on MMT reduction assay, the synthesized hydrogel was found to show no trace of cytotoxic effect on WRL 68 cell lines. The pH responsiveness of the hydrogels obtained from the synthesized macromer was studied in aqueous solution. Varying the amount of PEGMA during macromer

synthesis not only resulted in hydrogels with varied hydration rate, but also changes the thermal stability of the hydrogel. The experimental data demonstrated dependency of hydrogel's thermal stability and LCST on the hydrophilic PEGMA content of the macromer. Increasing the PEGMA fraction of the hydrogel from 10 to 50% resulted in increased T_d from 430 to 470°C. An increase in LCST from 29°C to the physiological temperature 37°C, which was the highest recorded LCST, was observed with hydrogel with 50% PEGMA content. The change in PEGMA content was also found to significantly influence the hydrogel's hydration rate (r) from 2.8×10^{-5} to 7.6×10^{-5} mL·s⁻¹. The hydrogel's equilibrium weight swelling ratio (q_e), protein release and its diffusion coefficient (D_m) were all found to be pH dependent. Increasing the buffer pH from 2.4 to 13 resulted in increased q_e from 2 to 16. This corresponded to the enlarged network mesh size (ξ) from 150 to 586 nm, with an increase in D_m from 1.4 to 2.7 cm²·s⁻¹. Increased amount of protein release from 0.6 to about 28 µg·mL⁻¹ was also obtained. The hydrogel crosslinker type was found to influence the flexibility and ductility of the hydrogel. The data presented herein contribute to the library of design parameters for novel pH responsive hydrogels that can be operated in microfluidic, muscle actuators or controlled release devices.

ACKNOWLEDGMENTS

The University of Malaya is acknowledged for funding this work through research grants BK014-2014, RP024-2012A, RU005B-2014, and UM.C/625/1/HIR/MOHE/05.

REFERENCES

1. Lee, V. H.; Yamamoto, A. *Adv. Drug Delivery Rev.* **1989**, *4*, 171.
2. Hennink, W. E.; Franssen, O.; van Dijk-Wolthuis, W. N. E.; Talsma, H. *J. Control. Release* **1997**, *48*, 107.
3. Schoener, C. A.; Hutson, H. N.; Peppas, N. A. *J. Biomed. Mater. Res. Part A* **2012**.
4. Johnson, B.; Beebe, D.; Crone, W. *Mater. Sci. Eng. C* **2004**, *24*, 575.
5. Techawanitchai, P.; Ebara, M.; Idota, N.; Asoh, T.-A.; Kikuchi, A.; Aoyagi, T. *Soft Matter* **2012**, *8*, 2844.
6. Kelley, E. G.; Albert, J. N.; Sullivan, M. O.; Epps III, T. H. *Chem. Soc. Rev.* **2013**, *42*, 7057.
7. Schillemans, J. P.; Verheyen, E.; Barendregt, A.; Hennink, W. E.; Van Nostrum, C. F. *J. Control. Release* **2011**, *150*, 266.
8. Lin, C.-C.; Anseth, K. S. *Pharm. Res.* **2009**, *26*, 631.
9. Koutsopoulos, S.; Unsworth, L. D.; Nagai, Y.; Zhang, S. *Proc. Natl. Acad. Sci. USA* **2009**, *106*, 4623.
10. Patterson, J.; Siew, R.; Herring, S. W.; Lin, A. S.; Gulberg, R.; Stayton, P. S. *Biomaterials* **2010**, *31*, 6772.
11. Bertz, A.; Wöhl-Bruhn, S.; Miethe, S.; Tiersch, B.; Koetz, J.; Hust, M.; Bunjes, H.; Menzel, H. *J. Biotechnol.* **2013**, *163*, 243.
12. Chen, X.; Martin, B. D.; Neubauer, T. K.; Linhardt, R. J.; Dordick, J. S.; Rethwisch, D. G. *Carbohydr. Polym.* **1995**, *28*, 15.
13. Vieira, E. F. S.; Cestari, A. R.; Airoidi, C.; Loh, W. *Biomacromolecules* **2008**, *9*, 1195.
14. Hu, C.-H.; Zhang, X.-Z.; Zhang, L.; Xu, X.-D.; Zhuo, R.-X. *J. Mater. Chem.* **2009**, *19*, 8982.
15. Suresh, S. *Acta Mater.* **2007**, *55*, 3989.
16. Li, J.; Li, X.; Ni, X.; Wang, X.; Li, H.; Leong, K. W. *Biomaterials* **2006**, *27*, 4132.
17. Berry, D. J.; DiGiovanna, C. V.; Metric, S.; Murugan, R. *Arkivoc* **2001**, *2*, 944.
18. Ghosh, S.; Chiang, P. C.; Wahlstrom, J. L.; Fujiwara, H.; Selbo, J. G.; Roberds, S. L. *Basic Clin. Pharm. Toxicol.* **2008**, *102*, 453.
19. Gumel, A. M.; Annuar, M. S. M.; Heidelberg, T. *PLoS One* **2012**, *7*, e45214.
20. Gumel, A. M.; Annuar, S. M.; Heidelberg, T. *J. Chem. Technol. Biotechnol.* **2013**, *88*, 1328.
21. Bradford, M. M. *Anal. Biochem.* **1976**, *72*, 248.
22. Zor, T.; Selinger, Z., *Anal. Biochem.* **1996**, *236*, 302.
23. Gumel, A. M.; Annuar, M. S. M.; Heidelberg, T. *Polym. Degrad. Stab.* **2012**, *97*, 1224.
24. Constantin, M.; Cristea, M.; Ascenzi, P.; Fundueanu, G. *Express Polym. Lett.* **2011**, *5*, 839.
25. Shin, H.; Temenoff, J. S.; Mikos, A. G. *Biomacromolecules* **2003**, *4*, 552.
26. Twentyman, P.; Luscombe, M. *Br. J. Cancer* **1987**, *56*, 279.
27. Wu, D.-Q.; Wang, T.; Lu, B.; Xu, X.-D.; Cheng, S.-X.; Jiang, X.-J.; Zhang, X.-Z.; Zhuo, R.-X. *Langmuir* **2008**, *24*, 10306.
28. Keys, K. B.; Andreopoulos, F. M.; Peppas, N. A. *Macromolecules* **1998**, *31*, 8149.
29. Peppas, N. A.; Hilt, J. Z.; Khademhosseini, A.; Langer, R. *Adv. Mater.* **2006**, *18*, 1345.
30. Hennink, W. E.; Talsma, H.; Borchert, J. C. H.; De Smedt, S. C.; Demeester, J. *J. Control. Release* **1996**, *39*, 47.
31. Merrill, E. W.; Dennison, K. A.; Sung, C. *Biomaterials* **1993**, *14*, 1117.
32. Gumel, A. M.; Annuar, M. S. M.; Chisti, Y. *Ultrason. Sonochem.* **2013**, *20*, 937.
33. Wang, K.; Xu, X.; Liu, T.; Fu, S.; Guo, G.; Gu, Y.; Luo, F.; Zhao, X.; Wei, Y.; Qian, Z. *Carbohydr. Polym.* **2010**, *79*, 755.
34. Gumel, A. M.; Annuar, M. S. M.; Heidelberg, T. *Int. J. Biol. Macromol.* **2013**, *55*, 127.
35. Wang, X.; Wu, Q.; Wang, N.; Lin, X. F. *Carbohydr. Polym.* **2005**, *60*, 357.
36. Draye, J.-P.; Delaey, B.; Van de Voorde, A.; Van Den Bulcke, A.; De Reu, B.; Schacht, E. *Biomaterials* **1998**, *19*, 1677.
37. Trudel, J.; Massia, S. *Biomaterials* **2002**, *23*, 3299.
38. Weber, L. M.; Lopez, C. G.; Anseth, K. S. *J. Biomed. Mater. Res. Part A* **2009**, *90*, 720.
39. Loh, X. J.; Zhang, Z.-X.; Wu, Y.-L.; Lee, T. S.; Li, J. *Macromolecules* **2008**, *42*, 194.
40. Li, J.; Li, X.; Ni, X.; Leong, K. W. *Macromolecules* **2003**, *36*, 2661.

41. Kim, J. H.; Sim, S. J.; Lee, D. H.; Kim, D.; Lee, Y. K.; Chung, D. J.; Kim, J.-H. *Polym. J.* **2004**, *36*, 943.
42. Zhang, X.-Z.; Chu, C.-C. *Polymer* **2005**, *46*, 9664.
43. Fournier, D.; Hoogenboom, R.; Thijs, H. M.; Paulus, R. M.; Schubert, U. S. *Macromolecules* **2007**, *40*, 915.
44. Mori, H.; Iwaya, H.; Nagai, A.; Endo, T. *Chem. Commun.* **2005**, 4872.
45. Dong, H.; Du, H.; Qian, X. *J. Phys. Chem. A* **2008**, *112*, 12687.
46. Donini, C.; Robinson, D. N.; Colombo, P.; Giordano, F.; Peppas, N. A. *Int. J. Pharm.* **2002**, *245*, 83.
47. Torres-Lugo, M.; Peppas, N. A. *Macromolecules* **1999**, *32*, 6646.
48. Eichenbaum, K. D.; Thomas, A. A.; Eichenbaum, G. M.; Gibney, B. R.; Needham, D.; Kiser, P. F. *Macromolecules* **2005**, *38*, 10757.
49. Jagadish, N. H.; Vishalakshi, B. *Der Pharma Chem.* **2012**, *4*, 946.